I&EC research
Industrial & Engineering Chemistry Research

pubs.acs.org/IECR

Article

Conversion of Pyrolysis Products into Volatile Fatty Acids with a Biochar-Packed Anaerobic Bioreactor

Yusuf Küçükağa, Andrea Facchin, Serdar Kara, Tülin Yılmaz Nayır, Daniel Scicchitano, Simone Rampelli, Marco Candela, and Cristian Torri*

Cite This: *Ind. Eng. Chem. Res.* 2022, 61, 16624−16634

Read Online

ACCESS | Metrics & More | Article Recommendations | Supporting Information

Downloaded via UNIV BOLOGNA on November 18, 2022 at 16:15:44 (UTC).
See https://pubs.acs.org/sharingguidelines for options on how to legitimately share published articles.

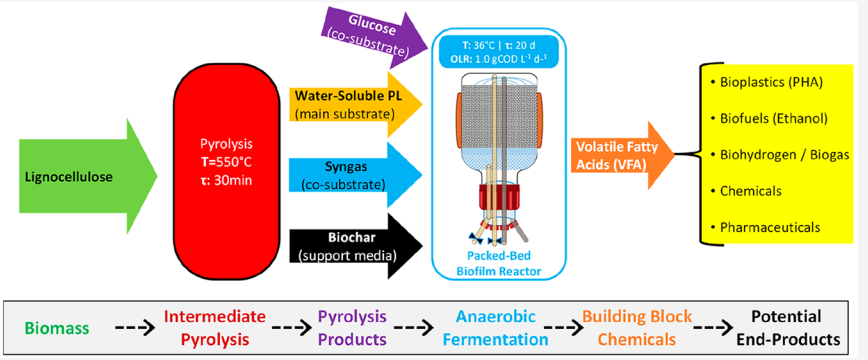

ABSTRACT: The coupling of pyrolysis and acidogenic fermentation was here proposed as a new hybrid thermochemical-biological method to circumvent the hydrolysis bottleneck within lignocellulose valorization schemes. Pyrolysis products of fir sawdust, that is, the water-soluble (WS) fraction together with CO-rich syngas, were tested as feedstock for volatile fatty acid (VFA) production. WS/syngas conversion to VFA was particularly challenging due to the combined effect of the substrate (WS/syngas) and product (VFA) inhibition. To solve such an issue, a new type of bioreactor, based on packed biochar and a new acclimatization/bioaugmentation procedure consisting of co-feeding WS/syngas and glucose were developed and tested. The gradual switch from glucose to WS was monitored through various analytical techniques, observing the transition toward a "pyrotrophic" microbial mixed culture able to convert WS/syngas into VFA. Even without selective inhibition of methanogens, the main fermentation products were VFA (mainly acetic, butyric, and caproic acid), whose profile was a function of the WS/glucose ratio. Although the achieved volumetric productivity was lower (<0.6 gCOD L^{-1} d^{-1}) than that observed in sugar fermentation, bioaugmented pyrotrophs could convert headspace CO, most of GC−MS detectable compounds (*e.g.*, anhydrosugars), and a significant portion of non-GC−MS detectable compounds of WS (*e.g.*, oligomers with MW < 1.45 kDa).

1. INTRODUCTION

Lignocellulosic biomass is a renewable and potentially sustainable raw material for obtaining value-added chemicals and bio-materials. However, due to its heterogeneous and refractory physicochemical structure, lignocellulose is not easily bioavailable for biological conversion processes. The depolymerization of the slowly biodegradable fractions of lignocelluloses can be achieved by pyrolysis, namely the heating at 350−600 °C in the absence of or with minimal oxygen, which can convert a large array of different feedstock into a vapor stream enriched in pyrolysis products (PyP: water, gas, and condensable organics) and a carbonaceous residue (char or biochar).[1] The main product of intermediate and fast pyrolysis is the liquid phase (*i.e.*, bio-oil, pyrolytic liquid, pyrolysis tar, *etc.*), which can be easily fractionated into water-soluble (WS) (aqueous phase) and water-insoluble (organic phase) fractions.

Although pyrolysis is a high-rate and reliable technology, the high temperature used in the process implies a low selectivity of the depolymerization reaction, with the production of a mixture that cannot be used as it is in drop-in applications.[2] One of the most interesting approaches for upgrading PyP is the hybrid thermochemical-biological (HTB) biorefinery, a "biological funnel"[3] that can decrease the complexity of pyrolysis products and unlock advanced utilization.[4]

Summing up all bioavailable constituents of PyP, namely, gas (raw gas or syngas) and WS fraction, pyrolysis can deliver more than half of the chemical energy of a biomass, providing a performance that is better than what can be obtained by means

Received: August 4, 2022
Revised: October 12, 2022
Accepted: October 14, 2022
Published: November 4, 2022

ACS Publications

© 2022 The Authors. Published by American Chemical Society

of hydrolysis-based scheme.[5] Syngas is biodegradable and can be converted anaerobically to various target chemicals like hydrogen, alcohols and VFAs.[6] The main issue related to syngas conversion is the low water solubility of CO and H_2 as well as the eventual presence of highly toxic contaminants (*e.g.*, hydrogen cyanide or NO_x),[7] which are typically more relevant for gasification-derived syngas.[8] HTB processing of WS, which is the most relevant bioavailable fraction of PyP, is definitely less studied. Such a mixture, whose composition is still under study, is made by volatile fatty acids (VFA), anhydrosugars (AS), hydroxyacetaldehyde, polar phenols (*e.g.*, di or tri-hydroxybenzenes), anhydro-oligosaccharides formed by cellulose ejection, humin-like matter, and hybrid oligomers formed by lignin and cellulose.[9−11] WS is bioavailable and partially biodegradable,[12,13] and selected fractions of WS (*e.g.*, AS and VFA) were successfully converted with HTB schemes by several authors.[14−18] Whole WS can be converted to methane by anaerobic digestion in 55−76% yield,[19,20] and healthy microbial consortia can degrade most of the GC−MS detectable portion of WS.[21−23]

The addition of biochar and the use of suitable microbial mixed consortia (hereafter called "pyrotrophs"[24]) allows us to exploit syngas and a large portion of WS organics for the production of biochemical intermediates.[18,23] In particular, whereas methanogenic activity could be selectively inhibited, pyrotrophs could be used to convert syngas/WS into VFA, which in turns can be used as chemical or biochemical building blocks for the production of several products.[25]

Till date, there is only one work in which the conversion of pyrolysis condensable compounds into VFA was optimized.[26] Lemos and co-workers fermented a solution of 11 gCOD L^{-1} (about 1% by weight) of pyrolysis liquid from fast pyrolysis of chicken beds; with 2 d of hydraulic residence time (HRT) at 30 °C, 6.2 gCOD L^{-1}as VFAs were obtained, corresponding to 54% yield and volumetric productivity equal to 3.1 gCOD L^{-1} d^{-1}. Such concentrations and productivities of VFA were suitable for direct polyhydroxyalkanoate (PHA) production using microbial mixed culture (MMC).[27] Therefore, the author tested a combined anaerobic−aerobic system, demonstrating a final yield of PHA of 19% and an overall volumetric productivity of 0.7 gCOD L^{-1} d^{-1}.

Besides the work of Lemos *et al.*,[26] several studies focused on WS biomethanation often reported a significant VFA accumulation in the system, even when biogas production was completely absent. Torri and Fabbri[18] and Hübner *et al.*[22] tested low-temperature WS from wood pyrolyzed at 400 °C (at 35 gCOD L^{-1}) and digestate pyrolyzed at 330 °C (at 30 gCOD L^{-1}) in a batch test for a long time, showing that such high concentrations inhibit the methane production, giving a significant acidogenic activity. In both cases, total VFA concentration increased during the process, suggesting a biological conversion of PyP into VFA. Although these studies were not optimized for VFA production, the overall VFA yields (29 and 41%, respectively) were significant, and the final concentration (about 10 gCOD L^{-1}) of VFA reached the level of self-inhibition of acidogenesis due to the toxicity of undissociated VFA. Hübner *et al.*[22] also tested a similar concentration of WS obtained at 420 and 530 °C, observing the inhibition of both methanogenic and acidogenic activity.

As a whole, the limited available literature suggests that it could be possible to convert WS into VFA, even if, at the best of the author's knowledge, continuous conversion of WS into VFA was never demonstrated. This work aimed to fill this research gap by investigating the coupling of pyrolysis and fermentation to produce VFA. To demonstrate the reliability of such coupling, all the bioavailable PyP, namely syngas and WS, were provided to a packed-bed biofilm reactor. Nonetheless, given the possible applications of clean syngas, the reactor was designed as a biofilter and targeted to the conversion of WS, the less valuable part of pyrolysis products, into a broth rich in VFA.

To establish the system's performance and confirm the pyrotrophic activity, the biodegradation of pyrolysis products and the yield of fermentation intermediates (VFA, methane, and other GC−MS detectable compounds) were quantified within a 4 month fully continuous test. The effect of acclimatization, biochar addition, and glucose-aided bioaugmentation was evaluated, highlighting the potential and pitfalls of converting WS into VFA.

2. MATERIALS AND METHODS

2.1. Pyrolysis of Lignocellulosic Biomass. WS and syngas used for the experiments were obtained through intermediate pyrolysis of fir sawdust with fixed bed pyrolyzer, as detailed in the Supporting Information.[28] At each run (Figure S1), 5 g of biomass feedstock was pyrolyzed at 550 °C for 30 min residence time. Biomass feedstock and each PyP were analyzed to determine its chemical oxygen demand (COD). COD yields of PyP were calculated from mass yield and COD of each PyP (Table 1). Syngas with a calculated COD of 440 (±55) mgCOD L^{-1}_{syngas}, obtained from the sequential batch pyrolysis was stored in laminated foil gas bags (Supel Inert Foil 1L) and repeatedly analyzed over time, to assess the stability of composition (Table 1). A pre-portioned concentrated WS stock solution (194.8 ± 4.8 gCOD L^{-1}) was stored refrigerated (−20 °C) and used throughout all the fermentation experiments. Being the WS an extremely complex mixture of chemicals,[29] their full characterization was beyond the scope of this work; a preliminary analytical characterization of WS was carried out according to Torri *et al.*[30] and shown in detail (Figure 1). WS molecular constituents, which were considered relevant for fermentation and/or were monitored during the experiment, were: acetic acid (5.5%, as gCOD/$gCOD_{WS}$), hydroxyacetaldehyde (4.5%), levoglucosan (2.9%), mannosan (1.4%), ethanediol (0.8%), catechol (0.3%), and 4-methyl-catechol (0.3%).

Table 1. COD Yields of Pyrolysis Products, Composition of the Syngas, and the Original WS Concentration

PyP yields	$\%_{COD}$	syngas: 13.5% (±1), WS: 34.5% (±5), PL: 14.4% (±3), biochar: 35.4% (±2)
syngas constituents	v/v	CO: 31% (±5), H_2: 0.4% (±1), CH_4 9% (±1), CO_2: 16% (±6), N_2: 61% (±5)
WS concentration	gCOD L^{-1}	194.8 (±4.8)

2.2. Fermentation Setup and Analytical Methods. Acidogenic fermentation tests were performed in a 500 mL pyrex bottle, with a four-port cap that was used upside down to have all connections submerged by the liquid. Detailed description of structure and setup of the arduino based reactor can be found elsewhere.[31] Briefly, the bottle was partially filled with glass balls (5 mm) to sustain the packed-bed of biochar. Biochar used as packing material was a pellet-type charcoal obtained from orchard pruning, provided by "Romagna Carbone s.n.c." (Italy).[32] Packed-bed bioreactor were previously inoculated with a digestate from an industrial anaerobic digester treating mainly grape pomace, distillery stillage, and wastewater

https://doi.org/10.1021/acs.iecr.2c02810
Ind. Eng. Chem. Res. 2022, 61, 16624−16634

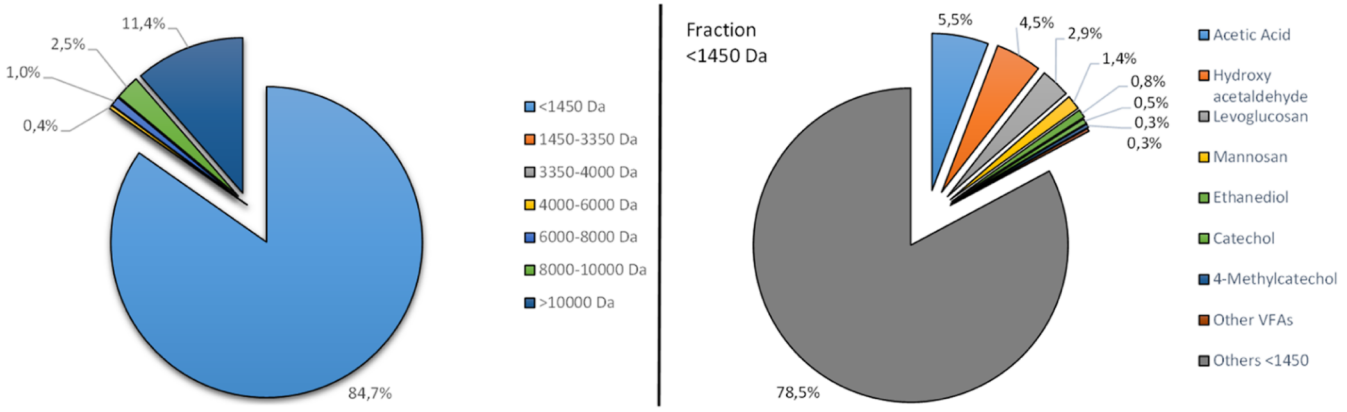

Figure 1. WS characterization: MW distribution by HPLC-SEC (left) and main GC−MS detectable compounds (right).

treatment sludges (supplied by Caviro Extra S.p.A., Faenza, Italy). The inoculum was a suspension with the following characteristics: pH 7.8, total COD 78.7 ± 0.7 gCOD L^{-1}, and suspended COD 74.0 ± 0.7 gCOD L^{-1}. A modified cultivation medium was prepared based on a study by Temudo *et al.*[31,33] (see Table S1). Nutrient supplementation was provided by assuming an average 5% microbial growth yield ($gCOD_{growth}$/$gCOD_{WS}$) and a C/N/P ratio of microbial biomass of 100:5:1. The equation used for estimating the required medium amount is provided in the Supporting Information together with all the other formulations that have been used in this study. Analytical characterization of the fermentation liquid output was carried out with COD analysis, size exclusion chromatography coupled with index of refraction detection (SEC-RID), and GC−MS using different derivatization and extraction techniques, according to Torri *et al.*[30]

2.3. 16S rRNA Gene Sequencing, Microbial Analysis, and SEM. At the end of each set of experiments, packed-bed bioreactors were rinsed with an excess amount of distilled water two times, and all the washing liquid was collected. Subsequently, the washing liquids were centrifuged for 15 min at 5000 rpm, the supernatant was discharged, and the precipitated sludge was collected. Additionally, the packing materials (biochar and glass bead) of the bioreactors were recovered at the end of the co-fermentation experiment. All microbial samples (sludge and packing material) were freeze-dried at −65 °C and 1.0 mbar vacuum conditions before the biological assays and scanning electron microscopy (SEM) analysis. Biochar samples were gold-coated before to SEM and photographed by Philips XL30S-FEG.

Total DNA was extracted from 500 mg of freeze-dried samples using the DNeasy PowerSoil Kit (QIAGEN, Hilden, Germany) following the manufacturer's instructions with a slight modification, and the homogenization step was performed in a FastPrep instrument (MP Biomedicals, Irvine, CA, United States) by three 1 min steps at 5.5 movements per sec. Total DNA was quantified by using NanoDrop ND-1000 (NanoDrop Technologies, Wilmington, DE), and 25 ng was used for the amplification step of the V3−V4 hypervariable region of the 16S rRNA gene using the 341F and 785R primers carrying Illumina adapter overhang sequences.[1] Briefly, the thermal cycle consisted of initial denaturation at 95 °C for 3 min, 25 cycles of denaturation at 95 °C for 30 s, annealing at 55 °C for 30 s, an elongation step at 72 °C for 30 s, and a final elongation step at 72 °C for 5 min. PCR products were purified by using Agencout AMPure XP magnetic beads (Beckman Coulter, Brea, CA), and the Nextera Technology was used to prepare indexed libraries by the limited cycle PCR reaction. After a further clean-up step as described above, libraries were normalized to 4 nM and pooled. The samples pool was denatured with 0.2 N NaOH and diluted to a final concentration of 6 pM with a 20% PhiX control. Sequencing was performed on the Illumina MiSeq platform using a 2 × 250 bp paired end protocol, according to the manufacturer's instructions (Illumina, San Diego, CA).

Raw microbial sequences were processed using a pipeline combining PANDASEQ[34] and QIIME2.[35] High-quality reads, obtained by a filtering step for length (min/max = 350/550 bp) and quality with default parameters in QIIME2, specifically, reads with an expected error per base E = 0.03 (*i.e.*, three expected errors every 100 bases) were discarded, based on the phred Q score probabilities. The resulted reads were clustered into amplicon sequence variants using DADA2.[36] Taxonomy was assigned using the VSEARCH algorithm[37] against SILVA database.[38] All the sequences assigned to eukaryotes (*i.e.*, chloroplasts and mitochondria) or unassigned were discarded. Microbial compositional analysis was performed using R software.

3. RESULTS AND DISCUSSION

3.1. Preliminary Tests and Setup of the Char-Bed Reactor. The efficacy of biochar as packing material for WS fermentation was verified by the preliminary fermentation tests, as shown in detail in the Supporting Information. The biochar-packed reactors resulted to be more effective and were less prone to intoxication than the glass ball-packed reactors; nonetheless, MMC could not address continuous WS biodegradation at a significant level without inhibition (>0.25 gCOD/L d). The inhibition was reversible with a total recovery of the process, testified by the disappearance of the main pyrolysis products (*e.g.* levoglucosan) after the stop of WS addition. The microbial inoculum can grow on PyP; therefore, it contained pyrotrophic microbes,[24] which are positively influenced by the biochar interaction, but the inhibition of biological activity occurred at a lower organic loading rate (OLR) than that demonstrated for stable biomethanation with a similar WS substrate.[18] These observations suggest a key role in the combined toxicity of WS and acidogenic fermentation products (VFA) and imply that the amount of VFA tolerant pyrotrophs should be drastically increased to obtain an acceptable volumetric productivity.

To increase the VFA tolerating pyrotrophs, a gradual bioaugmentation approach based on glucose/WS co-feeding and pH control (to pH = 6 Figure S8) was followed, aiming to

https://doi.org/10.1021/acs.iecr.2c02810
Ind. Eng. Chem. Res. 2022, 61, 16624−16634

Table 2. Operational Conditions Adopted in the Co-fermentation Experiment

parameters		phase I	phase II	phase III	phase IV	phase V	phase VI	overall
GLU/WS/syngas feed ratio	(% $_{gCOD:gCOD}$)	75:15:10	60:30:10	45:45:10	30:60:10	15:75:10	0:90:10	48:42:10
$COD_{SUBSTRATE}$	(gCOD L^{-1})	15 + 3 + 2	12 + 6 + 2	9 + 9 + 2	6 + 12 + 2	3 + 15 + 2	0 + 15 + 2	19.7
OLR	(gCOD L^{-1} d^{-1})	1.0	1.0	1.0	1.0	1.0	0.8	0.98
HRT	(d)	20	20	20	20	20	20	20
time	(d)	35[a]	21	21	14	14	9	114

[a]Including 9 days without COD input (batch period) due to operational issues.

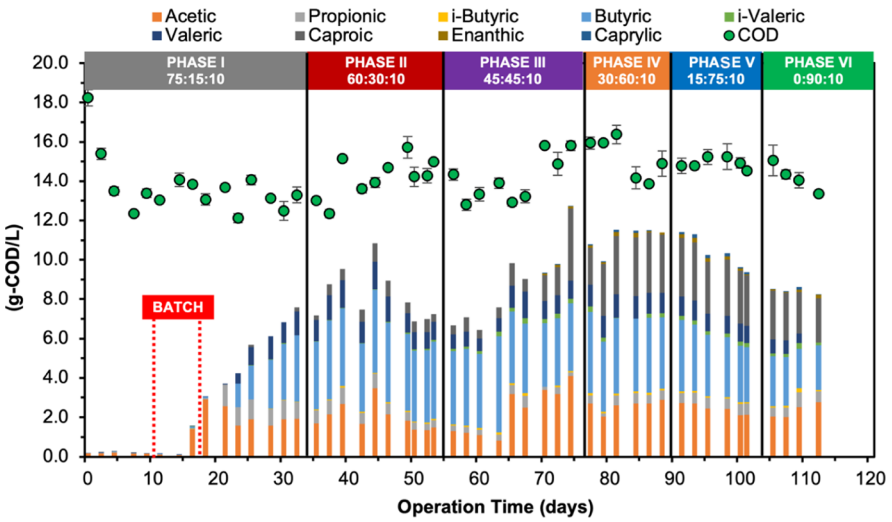

Figure 2. Total VFA concentration and COD profile in the experiment. All the operational phases with different feeding regimes and short-term no feeding period (batch) are marked on the graph.

first enrich a VFA tolerant MMC consortium and then select/acclimatize the pyrotrophs without the early intoxication phenomena observed for WS fermentation. Finally, to create a selective pressure toward a complete pyrotrophic MMC, syngas rich in CO (as an additional inhibitor) was added to the reactor headspace, providing a constant input of about 10% of the input COD. The operational conditions including the OLR (1.0 gCOD L^{-1} d^{-1}) were kept constant throughout the experiment, except for the input ratio between the co-substrates (Table 2). Different ratios of input materials were applied in six sequential operational phases with a gradual increase in the WS/glucose ratio in each phase. The biochar-packed bioreactor was operated in a continuous mode with 20 days of HRT, except for a very short period (hereinafter batch period) between the 11th and 18th days when the feeding was stopped.

3.2. Phase I (GLU 75%:WS 15%). Minimal biological activity was observed during the first 15 d of the experiment; meanwhile, a sharp increase in the acetic acid concentration was observed (Figure 2) together with a large production of CO_2 and a detectable CO consumption (Figure S7). The delay at the beginning of the fermentation was comparable to the typical lag phase observed in the presence of WS,[18] even if the stop in feeding between day 11 and day 18, which was due to operational issues, could have triggered the fermentation start, as previously observed in preliminary fermentation tests (Figure S5). After the stop in feeding, acidogenesis improved over time, with VFA concentrations that linearly increased from 3 to 7.5 gCOD L^{-1}. At the beginning of the experiment, acetic acid was the main VFA, while after 25 days, butyric acid become the most relevant VFA. The final amounts of acetic, propionic, butyric, valeric, and caproic acids at day 32 were 1.9, 0.8, 3.4, 1.2, and 0.2 gCOD L^{-1}, respectively.

Glucose and levoglucosan had a similar trend in the first phase of fermentation (Figure 3). Both started to be consumed after 15 days, gradually (glucose) or instantaneously (levoglucosan) reaching negligible concentrations in output solution. Mannosan, the main marker of hemicellulose pyrolysis, was consumed a few days later than levoglucosan and glucose, reaching a negligible amount in the output solution on day 25. This finding suggested a similar biodegradation rate for all the hexoses.

Ethanediol, a compound that can be formed during hydroxyacetaldehyde fermentation,[39] had a quite peculiar trend, with a gradual increase during the lag phase, followed by a sharp peak within the beginning of the acidogenic activity and a drop similar to that observed for sugars. Such a trend was similarly observed for phosphate, suggesting that both compounds can be considered as markers for MMC activity, which was characterized by an incomplete adaptation during the initial phase of WS degradation. The concentration of WS derived from lignin (catechol and 4-methylcatechol) slightly increased along with the WS input, suggesting an incomplete degradation of phenolics.

3.3. Phase II (GLU 60%:WS 30%). During the second phase of operation (+15% of WS in input, −15% glucose), the VFA concentration ranged between 6 and 11 gCOD L^{-1} (Figure 2), and their profile was stable (24% acetic, 7% propionic, 47% butyric, 14% valeric, and 7% caproic acid), in contrast to what happened in phase I. A significant increase in the production of CH_4 was observed (Figure S7); like the end of phase I, all sugars and ethanediol were not detected in the solution in output, whereas an almost constant concentration of catechol and 4-methylcatechol was observed. Phosphate (provided with the influent, see eq S1 in Supporting Information) was completely

https://doi.org/10.1021/acs.iecr.2c02810
Ind. Eng. Chem. Res. 2022, 61, 16624−16634

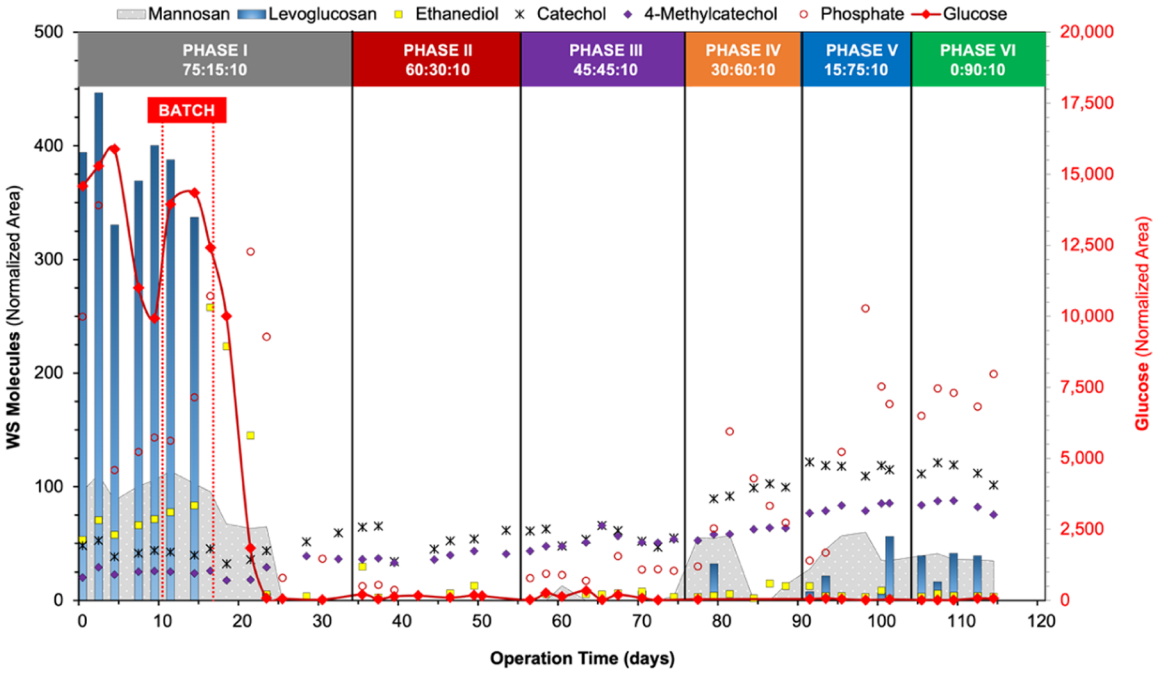

Figure 3. Profiles of normalized integrated area of the selected GC−MS detectable compounds in the solution in output. All the operational phases with different feeding regimes and short-term no feeding period (batch) are marked on the graph.

consumed, probably due to microbial growth (see eq S1 in Supporting Information).

3.4. Phase III (GLU 45%:WS 45%). Given the pyrotrophic activity reached during phase II, the substrate composition was further changed on day 56, providing the same amount of WS and glucose (45%) under the same operational conditions applied before. As result of time and feedstock change, the VFA concentration markedly increased to a final value of 12.8 gCOD L^{-1} (Figure 2) corresponding to 80% of the soluble COD of the solution in output. The VFA profile steeply changed as well, with a resulting relative content of acetic, propionic, butyric, valeric, and caproic acids of 32, 1, 27, 7, and 29%. The production of CH_4 and CO_2 was slightly higher than that of phase II (Figure S7), and higher consumption of CO was observed (2.2 mgCOD d^{-1}). GC−MS analyses of the solution in output showed a total consumption of all holocellulose derivatives analyzed and a slight increase in catechol and 4-methylcatechol almost proportional to the increase in WS share in the feeding. The phosphate concentration was slightly higher than what measured in phase II, suggesting a decreased biofilm formation rate that could be related to some stabilization of MMC.

3.5. Phase IV (GLU 30%:WS 60%). The WS concentration in the input solution was further increased during phase IV (12.0 gCOD L^{-1}). Even at a such high concentration of WS input, which was more than twice as compared to the previously tested concentrations in the mono-substrate fermentation test (see the Table S2 of Supporting Information), VFA concentrations in the solution in output were high and stable (11.5 gCOD L^{-1}), and VFA became the main soluble substances (≈80% of COD). As previously observed after each feedstock change, the VFA profile changed (Figure 2), with a further chain elongation: detectable amounts of enanthic and caprylic acids (C_7 and C_8) were observed, while caproic acid, which was almost absent using glucose-rich feedstock, became the second most dominant VFA type after butyric acid on COD basis. CH_4 and CO_2 production decreased (Figure S7), whereas the CO uptake was similar to the previous phase. The decreased methanogenesis activity can suggest that glucose was the preferential source for the residual methanogenic activity, and/or WS products selectively inhibited the residual methanogens. The decrease in CO_2 production could be expected by the fact that the COD/C ratio was higher for WS than that for glucose.

Levoglucosan was almost completely biodegraded (with a minor presence during day 79), while after more than 50 days without detecting holocellulose PyP, about 20% of the input concentration of mannosan was detected at the beginning of phase IV (Figure 3). Concentrations of phenols increased again similar to the increase in WS provided to the system.

Considering that most of COD during phase IV came from WS, the observed data trend suggested the end of biochar colonization and the appearance of phenomena more related to adaptation to inhibitors which, according to the higher feeding concentrations of WS, were well in the range for exerting toxicity. It was possible to identify a sort of "shock" on days 77−81 after the feedstock change, followed by another equilibrium (with a higher VFA concentration and lower levoglucosan and mannosan amounts) observed between day 81 and day 91.

3.6. Phase V (GLU 15%:WS 75%). WS concentration in the inlet was further increased to 17 gCOD L^{-1} during phase V, a much higher concentration than the highest concentration of non-treated/raw WS ever fermented (to the best of the authors' knowledge). Consequentially to the change in the substrate composition, VFA yield and concentration gradually decreased to 9.5 gCOD L^{-1} (Figure 2), while their profile did not change in comparison to phase IV. Given that just negligible amounts of anhydrosugars (levoglucosan on certain days and mannosan steadily) were detected in the solution in output, the decrease in the VFA yield, which can be probably related to WS overload, mainly affected the rate of conversion of non-GC detectable organics. Concerning lignin derivatives, 4-methylcatechol increased along with the increase in the WS input, whereas

https://doi.org/10.1021/acs.iecr.2c02810
Ind. Eng. Chem. Res. 2022, 61, 16624−16634

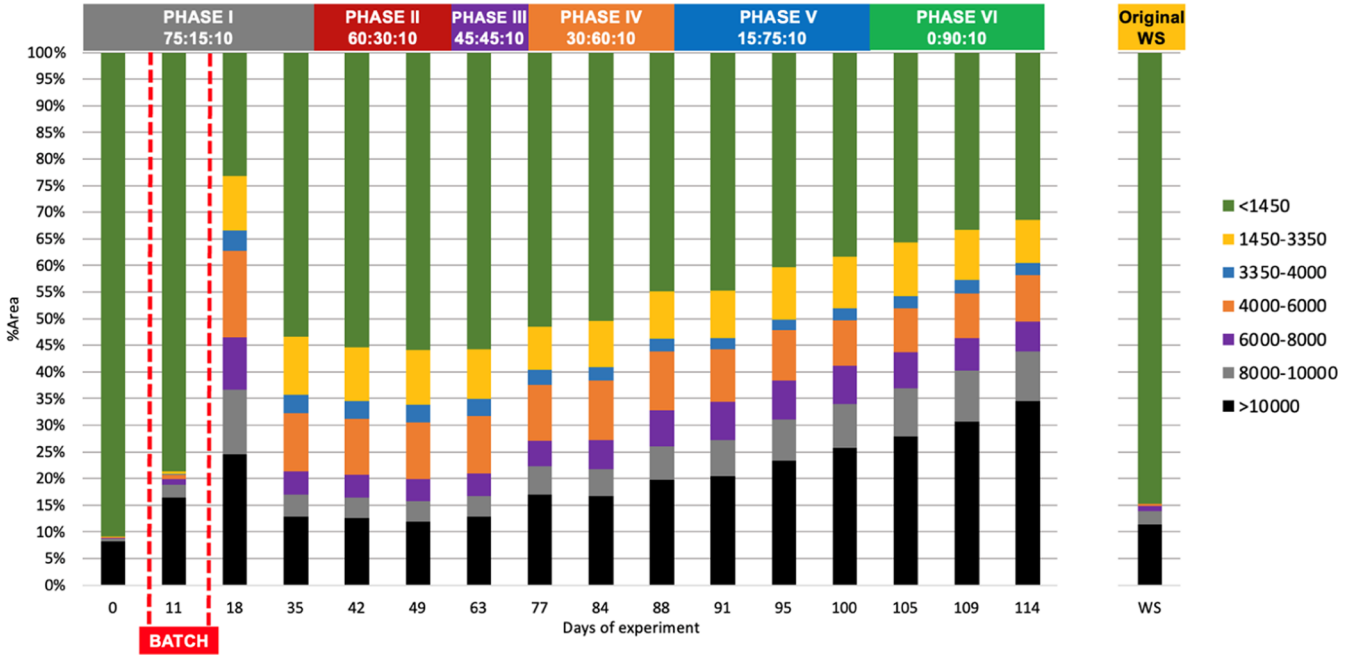

Figure 4. Molecular size distribution profile of the output solution obtained by HPLC-SEC (as in percentage area of RID detectable compounds). All the operational phases with different feeding regimes and short-term no feeding period (batch) are marked on the graph.

catechol had a constant concentration, suggesting a minimal degree of biodegradation.

3.7. Phase VI (GLU 0%:WS 90%). In the last phase, 17 gCOD L^{-1} as WS (90%) and syngas (10%) were the only feedstock provided to the bioreactor (Table 2). The VFA concentration (8.5 gCOD L^{-1}) stabilized on the value that was obtained at the end of phase V, whereas a decrease in the total COD from 15 to 13 gCOD L^{-1} of the outlet solution was observed as a consequence of glucose removal. Methane production was unchanged and the CO uptake was slightly improved to 2.3 mgCOD d^{-1}. Residual levoglucosan and mannosan were steadily detected by GC−MS by still achieving a highly efficient consumption of more than 95% of both anhydrosugars. On the other hand, both catechol and 4-methylcatechol had a decreasing trend soon after the phase switching. Although minimal, such an effect suggested that, after long bioaugmentation, pyrotrophic MMC can also biodegrade the WS phenols. However, biodegradability of WS phenols should be higlighted in longer-term studies.

3.8. SEC-RID Analysis of Output Solution. To obtain a general description of GC−MS detectable WS and non-analyzed constituents in terms of molecular weight (MW) distribution, the solution in output to the fermentation process was subjected to SEC-RID. The latter analysis did not reveal VFA and gave MW distribution (MWD) of sugar-like organics (*e.g.*, hydroxyacetaldehyde and anhydrosugars and sugars oligomers) and other WS compounds (*e.g.*, ethanediol and hydroxy acids) with an index of refraction higher than water. Therefore, the comparison of input and output MWD (Figure 4) is particularly useful to have information about WS fate without the limitation of GC−MS analysis.

MWD during the lag phase showed 80−90% relative content of low MW compounds (LMW < 1.45 kDa), mainly due to the unreacted glucose (Figure 4). Just after the lag phase (day 18) and glucose consumption, the solution in output consisted mainly of high MW compounds (HMW > 1450 Da), suggesting a preferential consumption of glucose and lighter WS organics in the beginning of the experiment (Figure 3).

Since glucose was never detected after day 25 (Figure 3) and VFA are not revealed by RID, the MWD can be mostly related to the unconverted portion of WS or polar constituents (*e.g.*, ethanediol) arising from the fermentative activity.

A clear and smooth transition toward HMW was observed during the experiment (Figure 4). In the beginning, roughly half of RID detectable constituents was made by LMW organics, 30% by compounds with MW between 1.45 and 10 kDa and only 20% by HMW compounds. Such a distribution was close to that of input WS, with partial removal of lighter compounds. Meanwhile, it was possible to see a decrease in the LMW concentration, an almost constant amount for organics with MW between 1.45 and 10 kDa, and a relative increase for MW > 10 kDa. At the end of phase VI, a mass distribution enriched in HMW organics (70% relative content) was observed. Since 70% of RID detectable organics in output had MW > 1.45 kDa, assuming that SEC-RID was representative of non-VFA organics (≈5 gCOD L^{-1} from Figure 2) and that all organics detected had a comparable COD, the final expected concentration of such compounds in output was about 3.5 gCOD L^{-1}. Such a value is very close to the expected inlet concentration of HMW, being 15% (Figure 2) of 17 gCOD L^{-1} provided as WS. Even if some changes in the relative distribution of HMW (enrichment of organics with MW between 1.45 and 10 kDa MW) occurred, the HMW seemed to enter the reactor without being consumed. The time trend of MW distribution observed during the experiment suggested that most of the compounds with MW < 1.45 kDa was increasingly converted during adaptation, whereas larger WS organics were not effectively converted by pyrotrophs. Such phenomena is not surprising considering that larger WS organics are characterized by chemical structures that are more challenging for biodegradation or, in some cases, known to be not biodegradable.[40]

3.9. Microbial Community Analysis: Pyrotrophs. Changes in the composition of the MMC were investigated by

https://doi.org/10.1021/acs.iecr.2c02810
Ind. Eng. Chem. Res. 2022, 61, 16624−16634

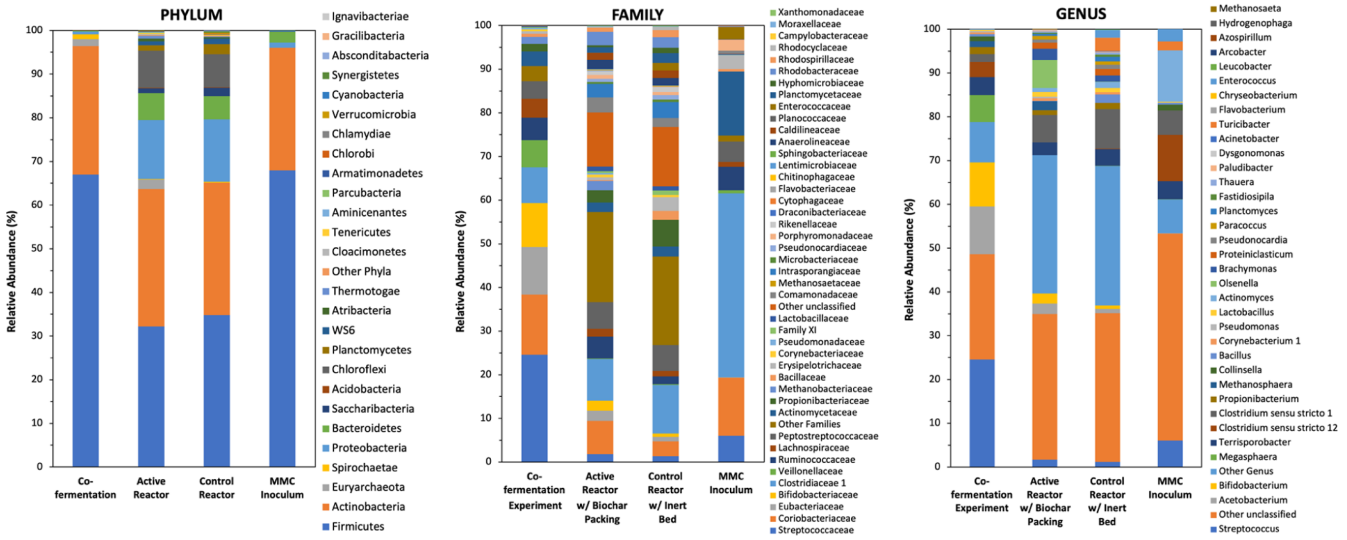

Figure 5. Taxonomic composition and r.a. of microbial communities found in biological samples (only phyla with a r.a. > 0.5% in at least one sample and families or genera with a r.a. > 1% in at least one sample are shown).

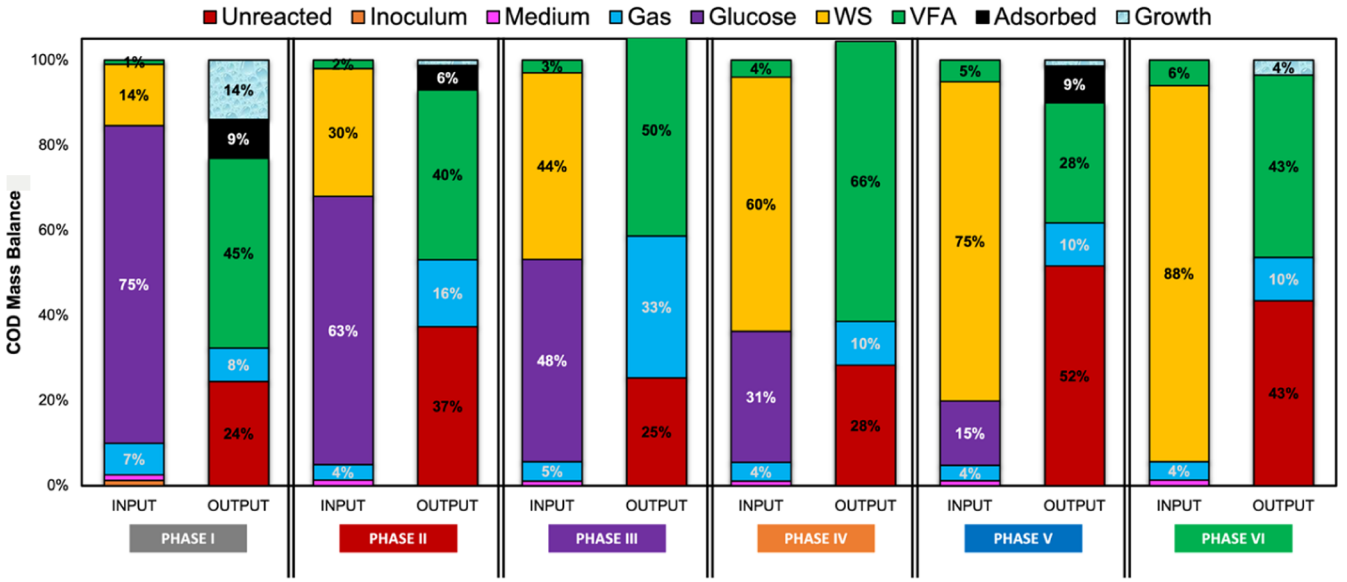

Figure 6. Overall COD balance for various phases of the co-fermentation experiment.

the next-generation sequencing method. The relative abundance (r.a.) at the phylum level (Figure 5) is showing that Firmicutes was the predominant type for all cases including the original seed sludge (inoculum), followed by Actinobacteria. The main differences obtained at the phylum level between reactors were for the third most dominant, which was Bacteroidetes for all the experiments except the co-fermentation experiment. On the other hand, the microbial abundance profiles were quite dissociated at the family level as compared to the phylum level, except for the mono-substrate tests which were quite similar to each other. The most dominant microbial family for the inoculum sludge was *Clostridiaceae*-1 with 42% r.a. However, *Streptococcaceae* with a 25% r.a. was dominating the sample from the co-fermentation experiment. In the case of samples from the mono-substrate tests having a large portion of other unclassified families, *Clostridiaceae*-1 is the most dominant classified family.

Total numbers of identified different genus types for co-fermentation, active reactor, control reactor, and inoculum that had a r.a. > 1% in at least one sample were 15, 26, 29, and 13, respectively. Moreover, a significantly lower percentage of "other genus" and "other unclassified" groups in the co-fermentation experiment (r.a. 33%) versus mono-substrate tests (r.a. ≈65%) was determined. Both these indications, implying a better microbial enrichment with livelier pyrotrophic consortia, have been achieved in the co-fermentation approach where glucose, WS, and syngas have been provided together to the biochar-packed bioreactor. *Streptococcus* was the most dominant genus type (r.a. 25%) in the co-fermentation experiment followed by *Acetobacterium* (r.a. 11%), *Bifidobacterium* (r.a. 10%), and *Megasphaera* (r.a. 6%). In the case of mono-substrate tests, most dominant genus types were varying from the co-fermentation experiment and also from each other. For instance, *Olsenella* and *Clostridium sensu stricto* 1 with 6% of r.a. ratios were the most dominant types in the active reactor (biochar-packed), while in the control reactor without biochar, anaerobic spore-forming *Clostridium sensu stricto 1* was the most dominant and only genus type with a r.a. of over 5%. This issue was implying that the fatty acid producer *Clostridium sensu stricto*

https://doi.org/10.1021/acs.iecr.2c02810
Ind. Eng. Chem. Res. 2022, 61, 16624−16634

1 can be the most robust pyrotrophic microbe with the capability of metabolizing a wide range of compounds including carbohydrates, amino acids, and some aromatics.[41] This particular genus could survive with WS as a single-energy source regardless of the presence of biochar as a microbial enhancement tool, while the case of non-spore-forming anaerobic *Olsenella* (a dominant genus only in the biochar-packed active reactor of the mono-substrate test) can be given as an example of the biochar selectivity on pyrotrophic communities.

Biochar is known as a highly porous conductive material, and several studies reported that microorganisms, such as methanogenic archaea and hydrophobic microbiota, could colonize the biochar microporosities[42−45] as those shown with 1000 and 250 magnifications (Figure S9). SEM images of biochar samples demonstrated the presence of coccus and bacillus with 0.5 and 6.5 μm lengths on the outer and inner (*e.g.*, carbonized wood vessels) surfaces of biochar. Geometrical shapes of SEM-detected microbes were consistent with those of the 10 most abundant genus identified using the microbial community analysis (Figure 5).

3.10. Overall Performance Evaluation. To prove the consistency of the experimental results and to highlight the effectiveness of WS conversion along the bioaugmentation, a COD balance was performed for all the operational phases. A glance at the COD input, namely glucose/WS/syngas, and outputs, namely gas, VFA, other soluble organics, adsorbed organics, and microbial growth are reported in Figure 6.

Product recovery rates on COD basis were acceptable all through the phases (Table S3). The lowest COD recovery was obtained in phase I, when 14% of the COD input was probably consumed for microbial growth (eq S14 in Supporting Information). After the microbial enrichment phase (which mainly occurred during Phase I), COD recoveries (COD_{out}/COD_{in}) were always above 90%.

Being the syngas just added to evaluate co-fermentation in a realistic system, most of the fermentation phenomena involved WS and glucose. Nonetheless, it was worth noticing that above 46% of fed CO was used: this was a quite promising performance for this bioreactor setup that was even not fully optimized for gas fermentation.

During phase I, in which most of the COD provided was from glucose, the main feature was an incomplete conversion of the COD in input (yield of unreacted was 25%, mainly unconverted glucose). The yield of unreacted compounds apparently increased to 37% during phase II, even if glucose and GC−MS detectable WS compounds were mostly consumed. Given the limited information about non-GC−MS detectable WS, it was not possible to determine whether such an increase was just due to a minimal biodegradation of the latter portion of WS (roughly 28% of the input), to the production of non-VFA fermentation products (*e.g.*, ethanol, accounted as "unreacted"), or to the combination of both.

The clearest improvement in the conversion of the unreacted portion was observed during phase III, when still half of the soluble COD was provided as glucose; 50% VFA yield was obtained as the minimum amount (25%) of unreacted compounds in the solution in output was observed, and a significant (33%) yield of methane was achieved.

The switch from phase III and phase IV (60% WS) steered the fermentation path from methanogenesis toward acidogenesis. Methane-rich off-gas yield settled at 10%, and the reactor provided the best VFA yield (66%) with just 28% yield of unreacted substances. According to OLR used, the performance observed during phase IV corresponded to the best volumetric productivity of VFA obtained, equal to 560 mgCOD L^{-1} d^{-1}.

Phase V showed a decrease in the VFA yield (to 28%) and an increase in unreacted material (52%) that can be interpreted as a sort of shock due to the increase in WS provided. Nonetheless, even if the subsequent phase VI involved pure WS feedstock, such shock ended, with VFA yield that increased to 43% and unreacted compounds yield that decreased to 43%.

Considering that residual glucose was negligible after day 25, it can be assumed that the unreacted components of phase II and phase VI mainly came from WS. Using that assumption and comparing the unreacted amount with the WS input, it was possible to highlight that during phase II, the unreacted COD was close to that of WS provided. This meant that, even if the GC−MS detectable compounds of WS were completely degraded, the overall pyrotrophic activity (utilization of WS/syngas) was not relevant for the COD balance.

The transition toward pyrotrophy occurred during phase III when the unreacted COD become just a half of the WS provided. The ratio between unreacted compounds and WS remained stable during phase IV, and increased during phase V, probably due to the aforementioned shock, and finally settled around 49% during the last phase in which WS and syngas were the only feedstock provided. Considering that the unreacted portion included also some non-VFA byproducts, such a value was not so far from what was expected considering the entire biodegradable fraction of WS.[12,28] This suggests that the long-term enrichment procedure here used, where a gradually increasing ratio of the PyP input was applied together with an easily biodegradable co-substrate (glucose), allowed a reproducible selection of a biologically efficient pyrotrophic community, which was able to produce VFA with significant concentrations. From GC−MS and SEC-RID analysis, such pyrotrophs mainly addressed the lighter constituents of WS (MW < 1.45 kDa) with negligible activity toward HMW (>1.45 kDa) constituents of WS. It is worth noticing that the phase V condition was qualitatively identical to that tested in preliminary fermentation experiments; therefore, it can be stated that the long bioaugmentation procedure allowed us to culture pyrotrophs that can tolerate high concentrations of both WS (as inhibitory substrates) and VFA (as inhibitory products).

4. CONCLUSIONS

Previous studies already demonstrated the existence of pyrotrophs, namely an MMC able to use pyrolysis products as the carbon source, which can funnel the complex mixture released by pyrolysis to obtain utilizable chemicals.

The aim of this work was to establish whether it is possible to obtain and exploit pyrotrophic acidogenic consortia, able to produce VFA starting from whole, non-pretreated, mixture of pyrolysis products.

Preliminary results confirmed that biochar boost MMC growth, especially when dealing with PyP, but mono-substrate fermentation for production of VFA was not successful with direct WS fermentation and natural inoculum. Even at OLR as low as 0.25 gCOD L^{-1} d^{-1}, WS fermentation failed to provide a stable VFA production, showing a reversible intoxication phenomena, which was attributed to the combined effect of product (VFA) and substrate (WS) inhibition. Searching for new VFA tolerant pyrotrophic consortium, the MMC was bioaugmented through co-fermentation with glucose. A new of reactor type, based on packed biochar, and a new acclimatization

https://doi.org/10.1021/acs.iecr.2c02810
Ind. Eng. Chem. Res. 2022, 61, 16624−16634

procedure, consisting in co-feeding WS and glucose and constant amount of syngas were developed and tested.

Although the achieved volumetric productivity was low (<0.6 gCOD L^{-1} d^{-1}), bioaugmented pyrotrophs demonstrated to be able to convert most of the GC−MS detectable constituents (*e.g.*, anhydrosugars) of WS, a significant portion of non GC−MS detectable constituents (*e.g.*, oligomers with MW < 1.45 Da) together with headspace CO. Even without selective inhibition of methanogen, the main fermentation products were VFA, whose profile was a function of the WS/glucose ratio.

Looking to whole results, this work provided a novel way for the simultaneous utilization of gas (syngas), liquid (WS), and solid (biochar) products of intermediate pyrolysis through the original biochar-packed anaerobic bioreactor. Such an approach may already be applied for the valorization of various toxic aqueous effluents of thermochemical processes (*e.g.*, pyrolysis, gasification, and hydrothermal liquefaction) and, in a broad perspective, it could be a useful tool to circumvent the lignocellulose hydrolysis step. Nonetheless, it should be pointed out that the absolute yield of VFA and productivity are lower than those observed with compounds obtainable from hydrolysis (*e.g.*, glucose). The performances of the biochar-packed bioreactor could be improved considering the following issues:

- MMC improved their performances over the time, mainly due to an improved colonization of the biochar bed with increasingly adapted microorganisms. Therefore, longer adaptation and acclimatization/bioaugmentation procedures with increasing OLR could further improve the volumetric productivity.
- Being 9% of input converted into CH_4, the selective inhibition of methanogenic archaea with chemicals or suitable experimental conditions could increase VFA yields.[46]
- Most of the yield loss was caused by a scarce conversion of HMW organics; therefore, pyrolysis can be optimized to decrease the yield of such compounds and increase the yield of lighter bioavailable molecules.

■ ASSOCIATED CONTENT

Supporting Information

The Supporting Information is available free of charge at https://pubs.acs.org/doi/10.1021/acs.iecr.2c02810.

Methodological details; formulas and calculations; WS mono-substrate fermentation (preliminary tests); and SEM of biochar packing material (PDF)

■ AUTHOR INFORMATION

Corresponding Author

Cristian Torri − *Department of Chemistry "Giacomo Ciamician", University of Bologna, Ravenna 48123, Italy;* orcid.org/0000-0001-5233-6786; Email: cristian.torri@unibo.it

Authors

Yusuf Küçükağa − *Department of Chemistry "Giacomo Ciamician", University of Bologna, Ravenna 48123, Italy; Environmental Engineering Department, Faculty of Engineering, Gebze Technical University, Kocaeli 41400, Turkey;* orcid.org/0000-0002-0214-6834

Andrea Facchin − *Department of Chemistry "Giacomo Ciamician", University of Bologna, Ravenna 48123, Italy*

Serdar Kara − *Environmental Engineering Department, Faculty of Engineering, Gebze Technical University, Kocaeli 41400, Turkey*

Tülin Yılmaz Nayır − *Environmental Engineering Department, Faculty of Engineering, Gebze Technical University, Kocaeli 41400, Turkey*

Daniel Scicchitano − *Department of Pharmacy and Biotechnology, University of Bologna, Bologna 40126, Italy*

Simone Rampelli − *Department of Pharmacy and Biotechnology, University of Bologna, Bologna 40126, Italy*

Marco Candela − *Department of Pharmacy and Biotechnology, University of Bologna, Bologna 40126, Italy;* orcid.org/0000-0001-7420-790X

Complete contact information is available at: https://pubs.acs.org/10.1021/acs.iecr.2c02810

Notes

The authors declare no competing financial interest.

■ ACKNOWLEDGMENTS

Y.K. acknowledges the YOK (Council of Higher Education of Turkey) for the financial support received for performing the experiments conducted within YUDAB international scholarship program. Y.K. also would like to thank TUBITAK (Scientific and Technological Research Council of Turkey) for the scholarship provided within 2214A PhD research fellowship program.

■ REFERENCES

(1) Wright, M. M.; Brown, T. Costs of Thermochemical Conversion of Biomass to Power and Liquid Fuels. In *Thermochemical Processing of Biomass*, Brown, R. Ed.; 2019.

(2) Schwartz, T. J.; Shanks, B. H.; Dumesic, J. A. Coupling Chemical and Biological Catalysis: A Flexible Paradigm for Producing Biobased Chemicals. *Current Opinion in Biotechnology*; Elsevier Ltd April 1, 2016; Vol. *38*, pp 54−62.

(3) Linger, J. G.; Vardon, D. R.; Guarnieri, M. T.; Karp, E. M.; Hunsinger, G. B.; Franden, M. A.; Johnson, C. W.; Chupka, G.; Strathmann, T. J.; Pienkos, P. T.; et al. Lignin Valorization through Integrated Biological Funneling and Chemical Catalysis. *Proc. Natl. Acad. Sci. U.S.A.* **2014**, *111*, 12013−12018.

(4) Brown, R. C. Hybrid Thermochemical/Biological Processing: Putting the Cart before the Horse? *Appl. Biochem. Biotechnol.* **2007**, *137−140*, 947−956.

(5) Torri, C.; Favaro, L.; Facchin, A.; Küçükağa, Y.; Rombolà, A. G.; Fabbri, D. Could Pyrolysis Substitute Hydrolysis in 2nd Generation Biomass Valorization Strategies? A Chemical Oxygen Demand (COD) Approach. *J. Anal. Appl. Pyrolysis* **2022**, *163*, 105467.

(6) Sun, X.; Atiyeh, H. K.; Huhnke, R. L.; Tanner, R. S. *Syngas Fermentation Process Development for Production of Biofuels and Chemicals: A Review. Bioresource Technology Reports*; Elsevier Ltd September, 2019; Vol. *7*.

(7) Xu, D.; Tree, D. R.; Lewis, R. S. The Effects of Syngas Impurities on Syngas Fermentation to Liquid Fuels. *Biomass Bioenergy* **2011**, *35*, 2690−2696.

(8) Tian, F. J.; Yu, J. L.; Mckenzie, L. J.; Hayashi, J. I.; Chiba, T.; Li, C. Z. Formation of NOx Precursors during the Pyrolysis of Coal and Biomass. Part VII. Pyrolysis and Gasification of Cane Trash with Steam. *Fuel* **2005**, *84*, 371−376.

(9) Kanaujia, P. K.; Sharma, Y. K.; Agrawal, U. C.; Garg, M. O. Analytical Approaches to Characterizing Pyrolysis Oil from Biomass. *TrAC—Trends in Analytical Chemistry*; Elsevier B.V., 2013; Vol. *42*, pp 125−136.

(10) Mettler, M. S.; Vlachos, D. G.; Dauenhauer, P. J. Top Ten Fundamental Challenges of Biomass Pyrolysis for Biofuels. *Energy Environ. Sci.* **2012**, *5*, 7797−7809.

(11) Pinheiro Pires, A. P.; Arauzo, J.; Fonts, I.; Domine, M. E.; Fernández Arroyo, A.; Garcia-Perez, M. E.; Montoya, J.; Chejne, F.; Pfromm, P.; Garcia-Perez, M. *Challenges and Opportunities for Bio-Oil Refining: A Review. Energy and Fuels*; American Chemical Society June, 2019; Vol. *33*, pp 4683−4720.
(12) Blin, J.; Volle, G.; Girard, P.; Bridgwater, T.; Meier, D. Biodegradability of Biomass Pyrolysis Oils: Comparison to Conventional Petroleum Fuels and Alternatives Fuels in Current Use. *Fuel* **2007**, *86*, 2679−2686.
(13) Campisi, T.; Samorì, C.; Torri, C.; Barbera, G.; Foschini, A.; Kiwan, A.; Galletti, P.; Tagliavini, E.; Pasteris, A. Chemical and Ecotoxicological Properties of Three Bio-Oils from Pyrolysis of Biomasses. *Ecotoxicol. Environ. Saf.* **2016**, *132*, 87−93.
(14) Basaglia, M.; Favaro, L.; Torri, C.; Casella, S. Is Pyrolysis Bio-Oil Prone to Microbial Conversion into Added-Value Products? *Renewable Energy* **2021**, *163*, 783−791.
(15) Buendia-Kandia, F.; Greenhalf, C.; Barbiero, C.; Guedon, E.; Briens, C.; Berruti, F.; Dufour, A. Fermentation of Cellulose Pyrolysis Oil by a Clostridial Bacterium. *Biomass Bioenergy* **2020**, *143*, 105884.
(16) Luque, L.; Oudenhoven, S.; Westerhof, R.; van Rossum, G.; Berruti, F.; Kersten, S.; Rehmann, L. Comparison of Ethanol Production from Corn Cobs and Switchgrass Following a Pyrolysis-Based Biorefinery Approach. *Biotechnol. Biofuels* **2016**, *9*, 242.
(17) Luque, L.; Westerhof, R.; Van Rossum, G.; Oudenhoven, S.; Kersten, S.; Berruti, F.; Rehmann, L. Pyrolysis Based Bio-Refinery for the Production of Bioethanol from Demineralized Ligno-Cellulosic Biomass. *Bioresour. Technol.* **2014**, *161*, 20−28.
(18) Torri, C.; Fabbri, D. Biochar Enables Anaerobic Digestion of Aqueous Phase from Intermediate Pyrolysis of Biomass. *Bioresour. Technol.* **2014**, *172*, 335−341.
(19) Yang, Y.; Heaven, S.; Venetsaneas, N.; Banks, C. J.; Bridgwater, A. V. Slow Pyrolysis of Organic Fraction of Municipal Solid Waste (OFMSW): Characterisation of Products and Screening of the Aqueous Liquid Product for Anaerobic Digestion. *Appl. Energy* **2018**, *213*, 158−168.
(20) Doddapaneni, T. R. K. C.; Praveenkumar, R.; Tolvanen, H.; Palmroth, M. R. T.; Konttinen, J.; Rintala, J. Anaerobic Batch Conversion of Pine Wood Torrefaction Condensate. *Bioresour. Technol.* **2017**, *225*, 299−307.
(21) Wen, C.; Moreira, C. M.; Rehmann, L.; Berruti, F. Feasibility of Anaerobic Digestion as a Treatment for the Aqueous Pyrolysis Condensate (APC) of Birch Bark. *Bioresour. Technol.* **2020**, *307*, 123199.
(22) Hübner, T.; Mumme, J. Integration of Pyrolysis and Anaerobic Digestion—Use of Aqueous Liquor from Digestate Pyrolysis for Biogas Production. *Bioresour. Technol.* **2015**, *183*, 86−92.
(23) Torri, C.; Pambieri, G.; Gualandi, C.; Piraccini, M.; Rombolà, A. G.; Fabbri, D. Evaluation of the Potential Performance of Hyphenated Pyrolysis-Anaerobic Digestion (Py-AD) Process for Carbon Negative Fuels from Woody Biomass. *Renewable Energy* **2020**, *148*, 1190−1199.
(24) Torri, C.; Rombolà, A. G.; Kiwan, A.; Fabbri, D. Biomass Processing via Thermochemical-Biological Hybrid Processes. In *Biomass Valorization: Sustainable Methods for the Production of Chemicals*; Ravelli, D., Samorì, C., Eds.; Wiley Online Library, 2021; pp 181−223.
(25) Shen Lee, W.; Seak May Chua, A.; Koon Yeoh, H.; Cheng Ngoh, G. *A Review of the Production and Applications of Waste-Derived Volatile Fatty Acids*, 2013.
(26) Moita Fidalgo, R.; Ortigueira, J.; Freches, A.; Pelica, J.; Gonçalves, M.; Mendes, B.; Lemos, P. C. Bio-Oil Upgrading Strategies to Improve PHA Production from Selected Aerobic Mixed Cultures. *N. Biotechnol.* **2014**, *31*, 297−307.
(27) Villano, M.; Valentino, F.; Barbetta, A.; Martino, L.; Scandola, M.; Majone, M. Polyhydroxyalkanoates Production with Mixed Microbial Cultures: From Culture Selection to Polymer Recovery in a High-Rate Continuous Process. *N. Biotechnol.* **2014**, *31*, 289−296.
(28) Campisi, T.; Samorì, C.; Torri, C.; Barbera, G.; Foschini, A.; Kiwan, A.; Galletti, P.; Tagliavini, E.; Pasteris, A. Chemical and Ecotoxicological Properties of Three Bio-Oils from Pyrolysis of Biomasses. *Ecotoxicol. Environ. Saf.* **2016**, *132*, 87−93.
(29) Stankovikj, F.; McDonald, A. G.; Helms, G. L.; Olarte, M. V.; Garcia-Perez, M. Characterization of the Water-Soluble Fraction of Woody Biomass Pyrolysis Oils. *Energy Fuel.* **2017**, *31*, 1650−1664.
(30) Torri, C.; Kiwan, A.; Cavallo, M.; Pascalicchio, P.; Fabbri, D.; Vassura, I.; Rombolà, A. G.; Chiaberge, S.; Carbone, R.; Paglino, R.; et al. Biological Treatment of Hydrothermal Liquefaction (HTL) Wastewater: Analytical Evaluation of Continuous Process Streams. *J. Water Proc. Eng.* **2021**, *40*, 101798.
(31) Küçükağa, Y.; Facchin, A.; Torri, C.; Kara, S. An Original Arduino-Controlled Anaerobic Bioreactor Packed with Biochar as a Porous Filter Media. *MethodsX* **2022**, *9*, 101615.
(32) Rombolà, A. G.; Meredith, W.; Snape, C. E.; Baronti, S.; Genesio, L.; Vaccari, F. P.; Miglietta, F.; Fabbri, D. Fate of Soil Organic Carbon and Polycyclic Aromatic Hydrocarbons in a Vineyard Soil Treated with Biochar. *Environ. Sci. Technol.* **2015**, *49*, 11037−11044.
(33) Temudo, M. F.; Kleerebezem, R.; van Loosdrecht, M. Influence of the PH on (Open) Mixed Culture Fermentation of Glucose: A Chemostat Study. *Biotechnol. Bioeng.* **2007**, *98*, 69−79.
(34) Masella, A. P.; Bartram, A. K.; Truszkowski, J. M.; Brown, D. G.; Neufeld, J. D. PANDAseq: Paired-End Assembler for Illumina Sequences. *BMC Bioinf.* **2012**, *13*, 31.
(35) Bolyen, E.; Rideout, J. R.; Dillon, M. R.; Bokulich, N. A.; Abnet, C. C.; Al-Ghalith, G. A.; Alexander, H.; Alm, E. J.; Arumugam, M.; Asnicar, F.; Bai, Y.; Bisanz, J. E.; Bittinger, K.; Brejnrod, A.; Brislawn, C. J.; Brown, C. T.; Callahan, B. J.; Caraballo-Rodríguez, A. M.; Chase, J.; Cope, E. K.; Da Silva, R.; Diener, C.; Dorrestein, P. C.; Douglas, G. M.; Durall, D. M.; Duvallet, C.; Edwardson, C. F.; Ernst, M.; Estaki, M.; Fouquier, J.; Gauglitz, J. M.; Gibbons, S. M.; Gibson, D. L.; Gonzalez, A.; Gorlick, K.; Guo, J.; Hillmann, B.; Holmes, S.; Holste, H.; Huttenhower, C.; Huttley, G. A.; Janssen, S.; Jarmusch, A. K.; Jiang, L.; Kaehler, B. D.; Kang, K. B.; Keefe, C. R.; Keim, P.; Kelley, S. T.; Knights, D.; Koester, I.; Kosciolek, T.; Kreps, J.; Langille, M. G. I.; Lee, J.; Ley, R.; Liu, Y.-X.; Loftfield, E.; Lozupone, C.; Maher, M.; Marotz, C.; Martin, B. D.; McDonald, D.; McIver, L. J.; Melnik, A. V.; Metcalf, J. L.; Morgan, S. C.; Morton, J. T.; Naimey, A. T.; Navas-Molina, J. A.; Nothias, L. F.; Orchanian, S. B.; Pearson, T.; Peoples, S. L.; Petras, D.; Preuss, M. L.; Pruesse, E.; Rasmussen, L. B.; Rivers, A.; Robeson, M. S.; Rosenthal, P.; Segata, N.; Shaffer, M.; Shiffer, A.; Sinha, R.; Song, S. J.; Spear, J. R.; Swafford, A. D.; Thompson, L. R.; Torres, P. J.; Trinh, P.; Tripathi, A.; Turnbaugh, P. J.; Ul-Hasan, S.; van der Hooft, J. J. J.; Vargas, F.; Vázquez-Baeza, Y.; Vogtmann, E.; von Hippel, M.; Walters, W.; Wan, Y.; Wang, M.; Warren, J.; Weber, K. C.; Williamson, C. H. D.; Willis, A. D.; Xu, Z. Z.; Zaneveld, J. R.; Zhang, Y.; Zhu, Q.; Knight, R.; Caporaso, J. G. Reproducible, Interactive, Scalable and Extensible Microbiome Data Science Using QIIME 2. *Nat. Biotechnol.* **2019**, *37*, 852−857.
(36) Callahan, B. J.; McMurdie, P. J.; Rosen, M. J.; Han, A. W.; Johnson, A. J. A.; Holmes, S. P. DADA2: High-Resolution Sample Inference from Illumina Amplicon Data. *Nat. Methods* **2016**, *13*, 581−583.
(37) Rognes, T.; Flouri, T.; Nichols, B.; Quince, C.; Mahé, F. VSEARCH: A Versatile Open Source Tool for Metagenomics. *PeerJ* **2016**, *4*, No. e2584.
(38) Quast, C.; Pruesse, E.; Yilmaz, P.; Gerken, J.; Schweer, T.; Yarza, P.; Peplies, J.; Glöckner, F. O. The SILVA Ribosomal RNA Gene Database Project: Improved Data Processing and Web-Based Tools. *Nucleic Acids Res.* **2012**, *41*, D590−D596.
(39) Jayakody, L. N.; Horie, K.; Hayashi, N.; Kitagaki, H. Engineering Redox Cofactor Utilization for Detoxification of Glycolaldehyde, a Key Inhibitor of Bioethanol Production, in Yeast Saccharomyces Cerevisiae. *Appl. Microbiol. Biotechnol.* **2013**, *97*, 6589−6600.
(40) Pinheiro Pires, A. P.; Arauzo, J.; Fonts, I.; Domine, M. E.; Fernández Arroyo, A.; Garcia-Perez, M. E.; Montoya, J.; Chejne, F.; Pfromm, P.; Garcia-Perez, M. *Challenges and Opportunities for Bio-Oil Refining: A Review. Energy and Fuels*; American Chemical Society June, 2019; Vol. *33*, pp 4683−4720.

https://doi.org/10.1021/acs.iecr.2c02810
Ind. Eng. Chem. Res. 2022, 61, 16624−16634

(41) Alou, M. T.; Ndongo, S.; Frégère, L.; Labas, N.; Andrieu, C.; Richez, M.; Couderc, C.; Baudoin, J. P.; Abrahão, J.; Brah, S.; et al. Taxonogenomic Description of Four New Clostridium Species Isolated from Human Gut: "Clostridium Amazonitimonense", "Clostridium Merdae", "Clostridium Massilidielmoense" and "Clostridium Nigeriense". *New Microbes New Infect.* **2018**, *21*, 128−139.
(42) Lü, F.; Luo, C.; Shao, L.; He, P. Biochar Alleviates Combined Stress of Ammonium and Acids by Firstly Enriching Methanosaeta and Then Methanosarcina. *Water Res.* **2016**, *90*, 34−43.
(43) Pytlak, A.; Kasprzycka, A.; Szafranek-Nakonieczna, A.; Grządziel, J.; Kubaczyński, A.; Proc, K.; Onopiuk, P.; Walkiewicz, A.; Polakowski, C.; Gałązka, A.; et al. Biochar Addition Reinforces Microbial Interspecies Cooperation in Methanation of Sugar Beet Waste (Pulp). *Sci. Total Environ.* **2020**, *730*, 138921.
(44) Zhao, W.; Yang, H.; He, S.; Zhao, Q.; Wei, L. A Review of Biochar in Anaerobic Digestion to Improve Biogas Production: Performances, Mechanisms and Economic Assessments. *Bioresour. Technol.* **2021**, *341*, 125797.
(45) Lokesh, S.; Kim, J.; Zhou, Y.; Wu, D.; Pan, B.; Wang, X.; Behrens, S.; Huang, C. H.; Yang, Y. Anaerobic Dehalogenation by Reduced Aqueous Biochars. *Environ. Sci. Technol.* **2020**, *54*, 15142−15150.
(46) Liu, H.; Wang, J.; Wang, A.; Chen, J. Chemical Inhibitors of Methanogenesis and Putative Applications. *Appl. Microbiol. Biotechnol.* **2011**, *89*, 1333−1340.

Recommended by ACS

Hydrothermal Liquefaction of Cornstalk by Reusing Pyroligneous Acid: Synergistic Effects on Biocrude Oil Formation and Solid Residue Accumulation

Yanmei Li, Peng Fu, *et al.*

DECEMBER 22, 2021
ENERGY & FUELS

READ

Conversion of High-Solids Hydrothermally Pretreated Bioenergy Sorghum to Lipids and Ethanol Using Yeast Cultures

Ming-Hsun Cheng, Vijay Singh, *et al.*

JUNE 14, 2021
ACS SUSTAINABLE CHEMISTRY & ENGINEERING

READ

Using Undigested Biomass Solid Leftovers from the Saccharification Process to Integrate Lignosulfonate Production in a Sugarcane Bagasse Biorefinery

Otto Heinz, André Ferraz, *et al.*

JUNE 02, 2022
ACS SUSTAINABLE CHEMISTRY & ENGINEERING

READ

Catalytic Fast Pyrolysis of Soybean Straw Biomass for Glycolaldehyde-Rich Bio-oil Production and Subsequent Extraction

Mudassir Hussain Tahir, Hassaan Anwer Rathore, *et al.*

DECEMBER 02, 2021
ACS OMEGA

READ

Get More Suggestions >

https://doi.org/10.1021/acs.iecr.2c02810
Ind. Eng. Chem. Res. 2022, 61, 16624−16634